

Solving Hamiltonian Cycle Problem using Quantum \mathbb{Z}_2 Lattice Gauge Theory

Xiaopeng Cui¹ and Yu Shi^{1,*}

¹*Department of Physics & State Key Laboratory of Surface Physics,
Fudan University, Shanghai 200433, China*

Abstract

The Hamiltonian cycle (HC) problem in graph theory is a well-known NP-complete problem. We present an approach in terms of \mathbb{Z}_2 lattice gauge theory (LGT) defined on the lattice with the graph as its dual. When the coupling parameter g is less than the critical value g_c , the ground state is a superposition of all configurations with closed strings of spins in a same single-spin state, which can be obtained by using an adiabatic quantum algorithm with time complexity $O(\frac{1}{g_c^2} \sqrt{\frac{1}{\epsilon} N_e^{3/2} (N_v^3 + \frac{N_e}{g_c})})$, where N_v and N_e are the numbers of vertices and edges of the graph respectively. A subsequent search for a HC among those closed-strings solves the HC problem. For some random samples of small graphs, we demonstrate that the dependence of the average value of g_c on $\sqrt{N_{hc}}$, N_{hc} being the number of HCs, and that of the average value of $\frac{1}{g_c}$ on N_e are both linear. It is thus suggested that for some graphs, the HC problem may be solved in polynomial time. A possible quantum algorithm using g_c to infer N_{hc} is also discussed.

* yushi@fudan.edu.cn

In computational complexity, an important yet unproven conjecture for classical computing is $P \neq NP$, where P represents the class of problems that can be solved in times polynomial in the sizes of the inputs, while NP is the shorthand for nondeterministic polynomial, representing the class of problems the solutions of which can be verified in polynomial times. P is a subset of NP . The factoring problem, which is to find the prime factors of an odd number, is in class NP , but is conjectured not to be in class P .

In quantum computing, the factoring problem is in class P , as it can be solved by using Shor's algorithm in polynomial times [1], suggesting that quantum computing is more powerful than classical computing. However, it cannot be concluded that $P=NP$ in quantum computing, because factoring, as a specific NP problem, is not a NP -complete (NPC) problem, to which any NP problem can be reduced to in polynomial time. If any NPC problem can be solved in polynomial time, so do all the NP problems and consequently $P=NP$.

Therefore, if there is a quantum algorithm of polynomial time for any NPC problem, it can be concluded that $P=NP$ in quantum computing. It is thus important to find quantum speedup of any NPC problem.

A well-known NPC problem is the HC problem [2]. On an undirected graph, which is made up of a number of vertices connected by a number of edges without directions [3], a HC is a cycle that visits each vertex exactly once. HC problem is to determine whether such a HC exists. So far the best classical algorithms include the so-called dynamic programming algorithm of time complexity $O(N_v^2 2^{N_v})$ [4] and a Monte Carlo algorithm of time complexity $O(1.657^{N_v})$ [5], both of which are exponential in the number of vertices N_v . Up to now there is neither quantum algorithm with P time complexity [6].

In this paper, we propose a new approach to HC problem and thus the problem of P versus NP . We transform the HC problem to a problem in quantum \mathbb{Z}_2 LGT [7, 8]. Gauge theory is the framework describing the fundamental interactions in particle physics, as well as strong correlations in condensed matter physics. LGT is an approach to gauge theories by discretizing the spacetime or space to a lattice. \mathbb{Z}_2 LGT is the simplest LGT. Recently quantum simulation has become a new approach to LGT, including \mathbb{Z}_2 LGT [9–12].

We regard a graph as the dual of a lattice, on which the \mathbb{Z}_2 LGT is defined. Thus each vertex of the graph maps to a plaquette in the lattice, each edge in the graph crosses a link in the lattice, and two adjacent vertices in the graph correspond to two adjacent plaquettes in the lattice. The length is not defined for each edge in the graph or each link in the lattice,

therefore the lattice can be deformed when needed. Thus an undirected unweighted graph of N_v vertices becomes the dual lattice of a lattice with N_v plaquettes. Depicted in Fig. 1 is an example, in which the graph becomes the dual lattice of a 3×3 square lattice, with periodic boundary condition, i.e. a topologically torus lattice.

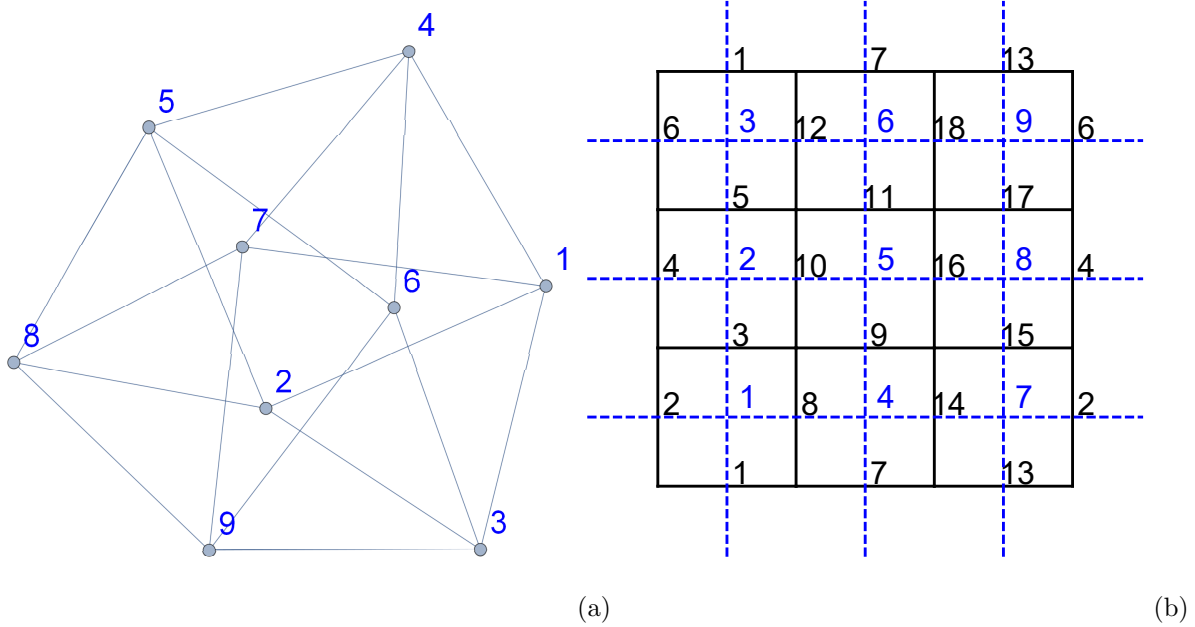


FIG. 1. Correspondence between a graph and the torus lattice. (a) A graph corresponding to the 3×3 torus lattice shown in (b). (b) 3×3 torus lattice, where the black solid lines are links of the lattice, the blue dotted lines correspond to the edges of the graph in (a), the numbers in black denote the edges of the lattice, and the numbers in blue correspond to those for the vertices in the graph in (a).

In this way, HC in a graph becomes HC in the dual lattice of a lattice. By connecting the last with the first visited vertices in the graph, an HC in the dual lattice becomes a closed string or loop passing through all the plaquettes of the lattice with periodic boundary condition, as shown in Fig. 2. Hence HC problem becomes the search for a closed string that visits each vertex of the dual lattice one. This is much easier, since the set of all the closed strings is much smaller than the set of all paths.

Furthermore, the search for a HC among the closed strings can be significantly accelerated by the topological quantum phase transition (TQPT) in the quantum \mathbb{Z}_2 LGT. At the critical value g_c of the coupling parameter g , a TQPT occurs separating the confined phase for $g > g_c$ and the deconfined phase for $g < g_c$, in which there is proliferation of the closed strings of

down spins, called closed-string condensation, as the ground state becomes a closed-string condensate, which is a quantum superposition of all configurations of closed strings of down spins (in the convention described below) [13, 14]. g_c depends on the properties of the graph, including N_{hc} , hence can be used to reveal N_{hc} . Therefore, reaching TQPT in a quantum adiabatic simulation becomes the key step in the present approach to HC problem. The dependence of g_c on N_{hc} suggests low time complexity, and to a new approach to the problem of P versus NP. This method applies to any graph, which can always be regarded as a dual lattice of a lattice, on which the \mathbb{Z}_2 LGT can always be defined.

Quantum \mathbb{Z}_2 LGT and closed strings.—The Hamiltonian of the quantum \mathbb{Z}_2 LGT [8, 11, 15] is

$$H = Z + gX \quad (1)$$

with

$$X = -\sum_l \sigma_l^x, Z = \sum_{\square} Z_{\square}, Z_{\square} = -\prod_{l \in \square} \sigma_l^z \quad (2)$$

where the spins (qubits) occupy the links l 's, \square represents the elementary plaquette of the lattice. Single-spin states $|0\rangle$ and $|1\rangle$ correspond to $\sigma_l^z = 1$ (up) and $\sigma_l^z = -1$ (down), respectively. The ground state at $g = 0$ is

$$|\psi_0\rangle = \sum_{i=1}^{S_0} |\phi_i\rangle, \quad (3)$$

where each $|\phi_i\rangle$ is with $Z_{\square} = -1$ for any \square and thus $Z = -9$. In the $M \times N$ torus lattice, there are $N_v \equiv MN$ plaquettes, $N_e \equiv 2N_v$ links. Hence the number of configurations with $Z = -9$ is $S_0 \equiv 2^{N_e}/(2^{N_v-1})$, where 2^{N_e} is the number of all possible configurations of spins, while $1/2^{N_v-1}$ is the probability that $Z_{\square} = -1$ for each \square .

On the dual lattice, one can regard a spin with $\sigma_l^z = -1$ as occupied by a string while a link with $\sigma_l^z = 1$ as unoccupied. Occupied links can be connected to form a longer string, which may be open or closed, then $|\phi_i\rangle$ can be regarded as a configuration of closed strings. When $g < g_c$, the ground state can be represented as a closed-string condensate, which is a superposition of S_0 configurations of closed strings. Especially, when $g = 0$, the superposition is of equal amplitude [13, 16, 17], Among the S_0 configurations of closed strings, two examples are as shown in the Fig. 2, where in (a), a single closed string passes through all N_v plaquettes of the lattice, and is thus a HC, while in (b), there are two closed strings, each passing through a part of the N_v plaquettes, so there is no HC.

Therefore, in order to solve HC problem, one only needs to search for HCs in the S_0 configurations of closed strings, rather than $N_v!$ configurations in the original configuration space [3]. This greatly reduces complexity.

Quantum Algorithm for HC problem. —The complexity of this quantum algorithm comes from the two consecutive processes. The first is to obtain the closed-string condensate, and the second is to search for HCs in it.

The initial state is the ground state at $g = +\infty$, which is the equal superposition of all product states of $|0\rangle$ and $|1\rangle$. With g decreased adiabatically towards $g \leq g_c$, the closed-string condensate is obtained. This process is equivalent to adiabatically evolve $H_\lambda = \lambda Z + X$, with $\lambda = \frac{1}{g}$, from $\lambda = 0$ towards $\lambda_c = \frac{1}{g_c}$.

The adiabatic condition implies that the time scale is $t = O(\sqrt{N_e})$ for a 2-dimensional lattice [18]. Hence the time scale is $t = O(\sqrt{N_e})\lambda_c$ for an lattice of an unknown λ_c .

For the adiabatic evolution, we use the symmetric Trotter decomposition to decompose the unitary evolution, which is more efficient than the original Trotter decomposition [19, 20]. The error for each step in the adiabatic simulation is $\varepsilon_s(t, n, g) = |e^{-i(A+B)t} - (e^{-iA\frac{t}{2n}}e^{-iB\frac{t}{n}}e^{-iA\frac{t}{2n}})^n| = |e^{-i(A+B)t} - e^{-iA\frac{t}{2n}}(e^{-iB\frac{t}{n}}e^{-iA\frac{t}{n}})^{n-1}e^{-iB\frac{t}{n}}e^{-iA\frac{t}{2n}}| \leq (\frac{1}{12}g^2N_vn_l^2 + \frac{1}{24}gN_e * n_p^2)\frac{t^3}{n^2}$, where $A = Z$ and $B = gX$ are the two terms in the Hamiltonian, t is time of the step, n is number of symmetric Trotter substeps, n_l is the number of links surrounding each plaquette, n_p is the number of vertices connected by each edge or is the number of plaquettes sharing each link [11]. Then the cumulative error from the start to the phase transition point λ_c can be obtained as

$$\varepsilon = O(\frac{1}{N_{ss}^2}N_e^{3/2}(N_v^3 + N_e\lambda_c)\lambda_c^4), \quad (4)$$

where N_{ss} is the total number of symmetric Trotter substeps. Therefore, the time complexity required in the adiabatic quantum simulation of the quantum \mathbb{Z}_2 LGT is

$$O_1 = O(\sqrt{\frac{1}{\varepsilon}N_e^{3/2}(N_v^3 + N_e\lambda_c)\lambda_c^4}) = O(\frac{1}{g_c^2}\sqrt{\frac{1}{\varepsilon}N_e^{3/2}(N_v^3 + \frac{N_e}{g_c})}), \quad (5)$$

where ε is reinterpreted as the precision required for the quantum simulation. In a connected undirected graph, $N_v \leq N_e \leq N_v(N_v - 1)/2$, g_c , λ_c are fixed quantities for a given graph.

Subsequently, a quantum search algorithm searches for HCs in the closed-string condensate, which is a superposition of $S_0 = O(2^{N_e}/2^{N_v})$ components, including those with HCs. The time complexity is $O_2 \sim \frac{S_0}{N_{hc}}$, since the probability of obtaining a state with a HC in a

measurement is $\frac{N_{hc}}{S_0}$. The relationship between N_{hc} and N_e of some sample graphs is shown in figure 10 (b). It is possible to develop a better quantum search algorithm finding HCs in the closed-string condensates. The time complexity for the whole process is $O = O_1 \cdot O_2$.

Quantum Algorithm of finding g_c .— g_c depends on and thus may reveal some properties of the graph, for example, N_{hc} . After reaching the TQPT, a measurement of g_c contributes additional time complexity O_M . According to the phase estimation method [11], O_M is of the same order of magnitude as O_1 . Thus with adiabatic algorithm followed by measurement, we have a quantum algorithm of finding g_c , with time complexity $O' = O_1 + O_M \sim O_1$.

Relations between g_c and the graph properties.—Because the complexity O_1 depends on $\lambda_c \equiv \frac{1}{g_c}$, we need to investigate the relations between g_c and the graph properties, e.g. N_{hc} and N_e .

We work on this problem using the classical demonstration of the quantum adiabatic simulation, in terms of the QuEST simulator [21]. The hardware we use is the Nvidia GPU Tesla V100-SXM2-32GB [11].

We first randomly generate four graphs with $N_v = 9$ and $N_e = 18$, as shown in Fig. 3(a-d). The fourth corresponds to the 3×3 torus lattice. N_{hc} of the four graphs are 0, 10, 30, 48, respectively. For such small graphs, we use measurement method, as described in [11], to obtain the ground state $|\psi_0\rangle$ at $g = 0$, as given in (3). Note that this method is not feasible for larger graphs, as in our discussion on the quantum algorithm for HC problems.

Then we adiabatically increase g from 0 to 1, in steps with $g_s = 0.001, t_s = 0.1, n = 100$, where g_s is the variation of g , t_s and n are the time and the number of the symmetric Trotter substeps within each step, respectively. The total cumulative error is $\varepsilon_{all} = \sum_{g=g_s}^1 \varepsilon_s(t, n, g)$, which is less than 0.135% for the graphs studied here. We study quantum phase transitions on the lattices corresponding to these graphs. First, $\langle H \rangle$, $\langle Z \rangle$ and $\langle Z \rangle$ are obtained as functions of g . Then we define two critical parameters, which are easily determined, to represent the critical parameter g_c . One is the extremal point g_c^H of the second derivative of $\langle H \rangle$, the other is the extremal point g_c^Z of the first derivative of $\langle Z \rangle$. $\lambda_c^H = \frac{1}{g_c^H}$, $\lambda_c^Z = \frac{1}{g_c^Z}$. As can be observed in Fig. 4(c-d), g_c^H and g_c^Z both increase with N_{hc} . This verifies that the properties of the graph directly affect the characteristics of the quantum phase transition.

In order to study how g_c^H and g_c^Z depend on N_{hc} , we prepare two groups of undirected and unweighted connected graphs with $N_v = 9$. The first group consists of 1000 samples, each with $N_e = 18$. We make the classical GPU demonstration of the adiabatic quantum

simulation, and obtained N_{hc} for each graph. The distribution of N_{hc} is shown in Fig. 5(a). The second group consists of 200 graphs for each value of N_e varying from 16 to 22. The distribution of N_{hc} is shown in the Fig. 5(b).

It can be seen from Fig. 6 that the average value of g_c^H and g_c^Z increase steadily with N_{hc} when N_e is fixed. Especially, when $N_{hc} = 0$, g_c^H and g_c^Z are very small. This shows that N_{hc} has a significant effect on g_c . This effect can help determine N_{hc} without searching the HCs of the graph. The time complexity required to reach TQPT is O_1 . g_c^H and g_c^Z may decrease linearly with N_e , as discussed below. Together with $N_v \leq N_e \leq N_v(N_v - 1)/2$, these properties imply that HC problem in these small graphs can be solved in polynomial time.

We have also studied the effect of N_e on the critical parameters, by using the second group of graphs with the same N_v value but different N_e values. As can be seen in the Fig. 7, the average values of g_c^H and g_c^Z decrease steadily with N_e when N_v is fixed. The larger the N_e value, the smaller the critical parameters. In other words, the average value of $\lambda_c = \frac{1}{g_c}$ increase linearly with N_e when N_v is fixed. Thus O_1 increases with N_e polynomially. On average, when N_v is fixed, the connectivity between vertices of a graph is proportional to N_e .

As can be seen in Fig. 8, when N_e and N_v are fixed, the average values of the critical parameters decrease with the maximal degree of the vertices $Max(Deg)$, while increases with the minimal degree of the vertices $Min(Deg)$. On average, when N_v and N_e are fixed, the larger $Max(Deg)$, the smaller ($Min(Deg)$). So the results in Fig. 8(a,c) and Fig. 8(b,d) are consistent.

Furthermore, we find that the relation between the average values of g_c^H and N_{hc} can be very well fitted quantitatively as

$$g_c^H = A\sqrt{N_{hc}} + B, \quad (6)$$

as shown in Fig. 9 for the two groups of graph samples. On the other hand, the relation between λ_c^H and N_e can be very well fitted as

$$\lambda_c^H = 0.1513 * N_e + 0.007536, \quad (7)$$

as shown in Fig.10. (6) and (7) are consistent. Due to the limitation of computing power, N_e is still relatively small in our simulated graphs, so the linear relationship needs verification in larger graphs.

In conclusion, we develop a novel approach to graph problem, by defining \mathbb{Z}_2 LGT on the lattice of which the graph is the dual lattice. Moreover, we present a quantum adiabatic algorithm with time complexity $O(\frac{1}{g_c^2} \sqrt{\frac{1}{\varepsilon} N_e^{3/2} (N_v^3 + \frac{N_e}{g_c})})$, to obtain the closed-string condensate emerging at the TQPT of the \mathbb{Z}_2 LGT, and find that the HC number N_{hc} of in the graph has a significant effect on the TQPT critical parameter g_c , providing a novel quantum algorithm for HC problem. Thereby a new approach to HC problem and P versus NP in quantum computing is proposed. Given the importance of graph theory in mathematics and computer science, our approach may also be useful to, say, deep learning, represented by deep neural networks and are being integrated with graphical models [22, 23], as well as quantum deep learning [24, 25]. This work also suggests a new direction of research connecting graph problems with topological quantum matter.

This work was supported by National Natural Science Foundation of China (Grant No. 12075059).

-
- [1] P. W. Shor, “Algorithms for quantum computation: discrete logarithms and factoring,” in *Proceedings 35th Annual Symposium on Foundations of Computer Science* (1994) pp. 124–134.
 - [2] J. van Leeuwen, ed., *Handbook of Theoretical Computer Science (Vol. B): Formal Models and Semantics* (MIT Press, Cambridge, MA, USA, 1991).
 - [3] M. R. Garey and D. S. Johnson, *Computers and Intractability; A Guide to the Theory of NP-Completeness* (W. H. Freeman & Co., USA, 1990).
 - [4] R. Bellman, “Dynamic programming treatment of the travelling salesman problem,” *J. ACM* **9**, 61 (1962).
 - [5] A. Björklund, “Determinant sums for undirected hamiltonicity,” in *2010 IEEE 51st Annual Symposium on Foundations of Computer Science* (2010) pp. 173–182.
 - [6] Anuradha Mahasinghe, Richard Hua, Michael J. Dinneen, and Rajni Goyal, “Solving the hamiltonian cycle problem using a quantum computer,” in *Proceedings of the Australasian Computer Science Week Multiconference, ACSW 2019* (Association for Computing Machinery, New York, NY, USA, 2019).

- [7] J. B. Kogut, “An introduction to lattice gauge theory and spin systems,” *Rev. Mod. Phys.* **51**, 659 (1979).
- [8] S. Sachdev, “Topological order, emergent gauge fields, and fermi surface reconstruction,” *Rep. Prog. Phys.* **82**, 014001 (2018).
- [9] S. Lloyd, “Universal quantum simulators,” *Science* **273**, 1073 (1996).
- [10] E. Zohar, A. Farace, B. Reznik, and J. I. Cirac, “Digital quantum simulation of $z(2)$ lattice gauge theories with dynamical fermionic matter,” *Phys. Rev. Lett.* **118**, 5 (2017).
- [11] X. Cui, Y. Shi, and J. C. Yang, “Circuit-based digital adiabatic quantum simulation and pseudoquantum simulation as new approaches to lattice gauge theory,” *J. High Energy Phys* **2020**, 160 (2020).
- [12] H. Lamm, S. Lawrence, and Y. Yamauchi (NuQS Collaboration), “General methods for digital quantum simulation of gauge theories,” *Phys. Rev. D* **100**, 034518 (2019).
- [13] M. A. Levin and X. G. Wen, “String-net condensation: A physical mechanism for topological phases,” *Phys. Rev. B* **71**, 045110 (2005).
- [14] X. G. Wen, “An introduction to quantum order, string-net condensation, and emergence of light and fermions,” *Ann. Phys.* **316**, 1 (2005).
- [15] F. J. Wegner, “Duality in generalized ising models and phase transitions without local order parameters,” *J. Math. Phys.* **12**, 2259 (1971).
- [16] M. Freedman, “A magnetic model with a possible chern-simons phase,” *Commun. Math. Phys.* **234**, 129183 (2003).
- [17] E. Fradkin, *Field Theories of Condensed Matter Physics* (Cambridge University Press, Cambridge, 2013).
- [18] A. Hama and D. A. Lidar, “Adiabatic preparation of topological order,” *Phys. Rev. Lett.* **100**, 4 (2008).
- [19] H. F. Trotter, “On the product of semi-groups of operators,” *Proc. Am. Math. Soc.* **10**, 545 (1959).
- [20] A. M. Childs, Y. Su, M. C. Tran, N. Wiebe, and S. Zhu, “A Theory of Trotter Error,” arXiv e-prints, arXiv:1912.08854 (2019).
- [21] T. Jones, A. Brown, I. Bush, and S. C. Benjamin, “QuEST and High Performance Simulation of Quantum Computers,” *Sci. Rep.* **9**, 10736 (2019).
- [22] M. J. Johnson, D. Duvenaud, A. B. Wiltschko, S. R. Datta, and R. P. Adams, “Composing

- graphical models with neural networks for structured representations and fast inference,” arXiv e-prints , arXiv:1603.06277 (2016).
- [23] H. Wang and D. Yeung, “Towards bayesian deep learning: A framework and some existing methods,” *IEEE Trans. Knowl. Data Eng.* **28**, 3395 (2016).
- [24] M. H. Amin, E. Andriyash, J. Rolfe, B. Kulchytskyy, and R. Melko, “Quantum boltzmann machine,” *Phys. Rev. X* **8**, 021050 (2018).
- [25] J. Biamonte, P. Wittek, N. Pancotti, P. Rebentrost, N. Wiebe, and S. Lloyd, “Quantum machine learning,” *Nature* **549**, 195–202 (2017).

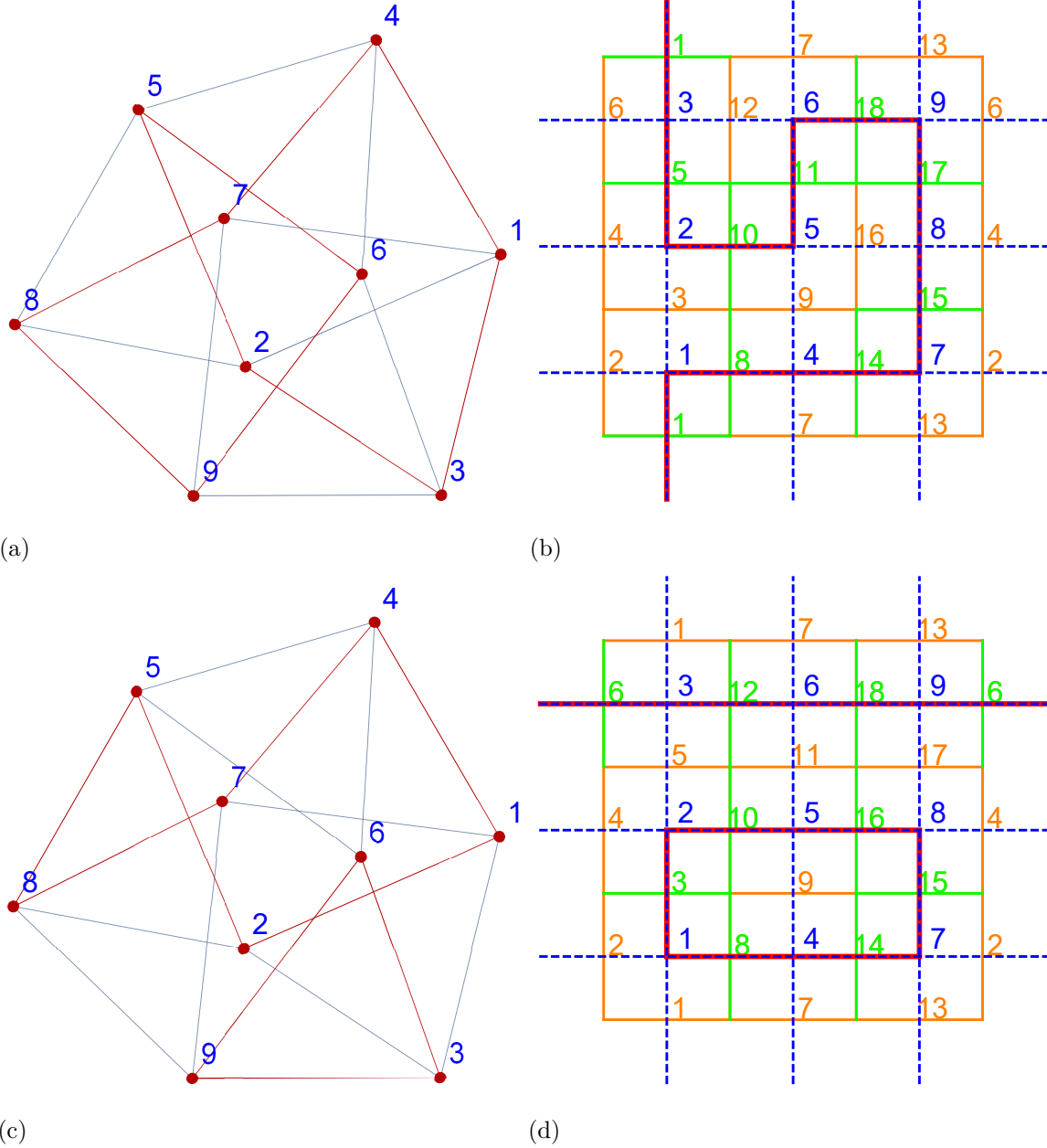


FIG. 2. Identification of the cycles on a certain graph as the closed strings on the dual lattice of a square lattice. (a) A HC of the graph, depicted as a red path in (a) becomes a closed string passing through all the plaquettes on the lattice, as depicted in red in (b). (b) A configuration of closed strings at the ground state of quantum \mathbb{Z}_2 LGT at $g = 0$. There is only one closed string, depicted as a red path. The orange edge is in the $|0\rangle$ state, and the green edge is in the $|1\rangle$ state. (c) Two cycles, depicted in red, in the graph. (d) A closed string configuration in the quantum \mathbb{Z}_2 LGT ground state at $g = 0$, with two closed strings, depicted as red paths, corresponding to the two cycles in the graph. The orange edge is in the $|0\rangle$ state, and the green edge is in the $|1\rangle$ state.

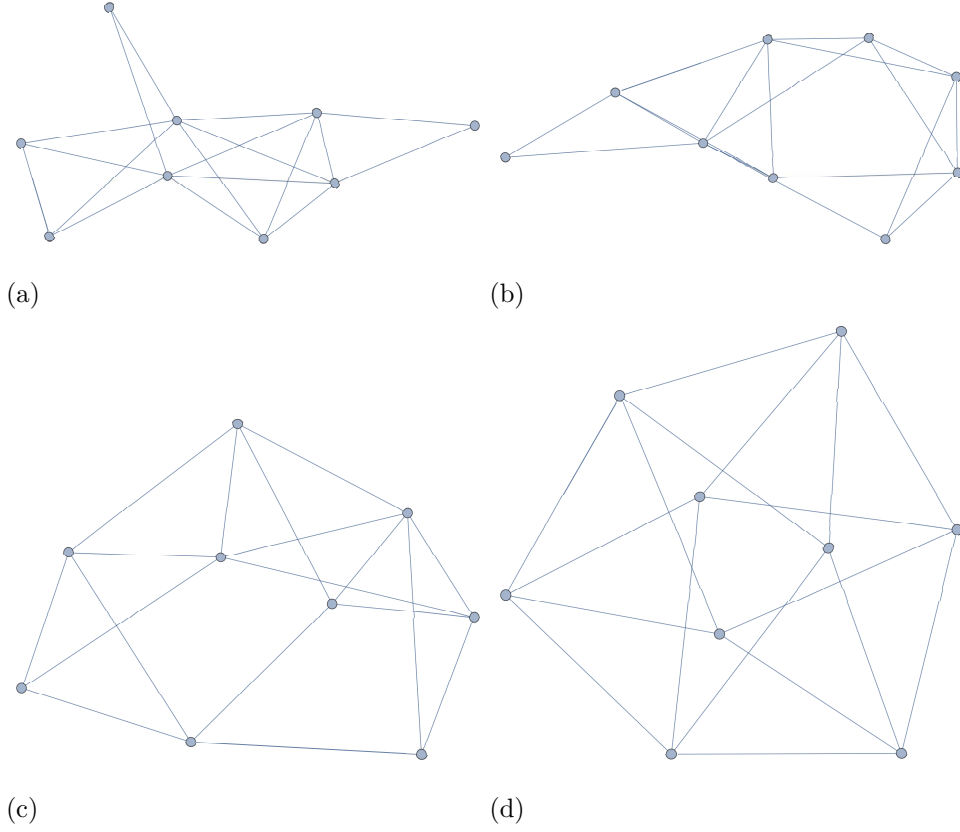


FIG. 3. Four different graphs used in calculating the critical parameters of the TQPT of \mathbb{Z}_2 LGT. (a) $G_1 : N_v = 9, N_e = 18, N_{hc} = 0$. (b) $G_2 : N_v = 9, N_e = 18, N_{hc} = 10$. (c) $G_3 : N_v = 9, N_e = 18, N_{hc} = 30$. (d) G_4 : the graph corresponding to the 3×3 torus lattice, $N_v = 9, N_e = 18, N_{hc} = 48$.

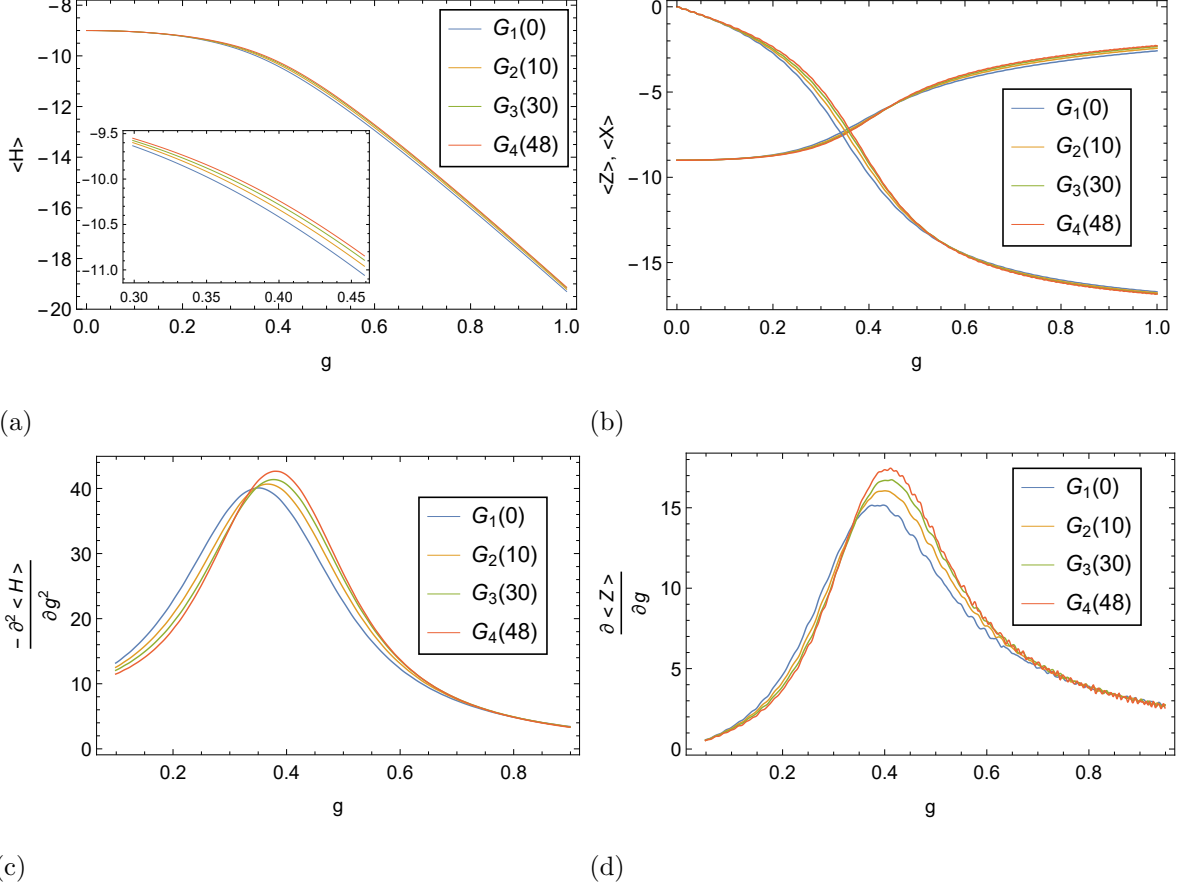


FIG. 4. (a) $\langle H \rangle$ for four graphs denoted in terms of N_{hc} . (b) $\langle Z \rangle$ and $\langle X \rangle$ for four graphs denoted in terms of N_{hc} . (c) The second derivatives of $\langle H \rangle$ for the four graphs, which can be used to determine the values of g_c^H . (d) The first derivative of $\langle Z \rangle$ for the four graphs, which can be used to determine the values of g_c^Z .

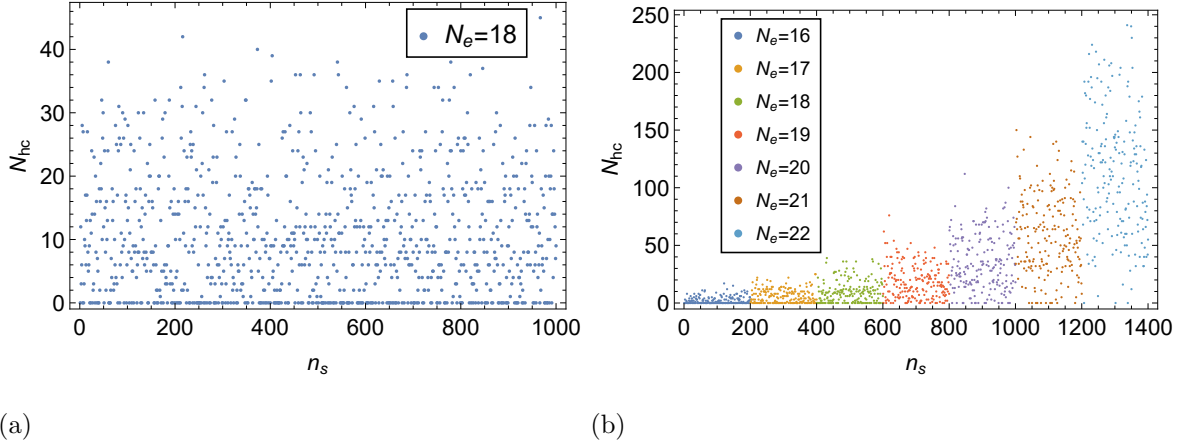


FIG. 5. Distribution of the N_{hc} among samples of graphs. n_s represents the number of the samples. (a) The case in which $N_e = 18$ in each sample. There are 1000 samples in total. (b) The case in which N_e varying from 16 to 22. There are 200 samples with each value of N_e , and 1400 samples in total.

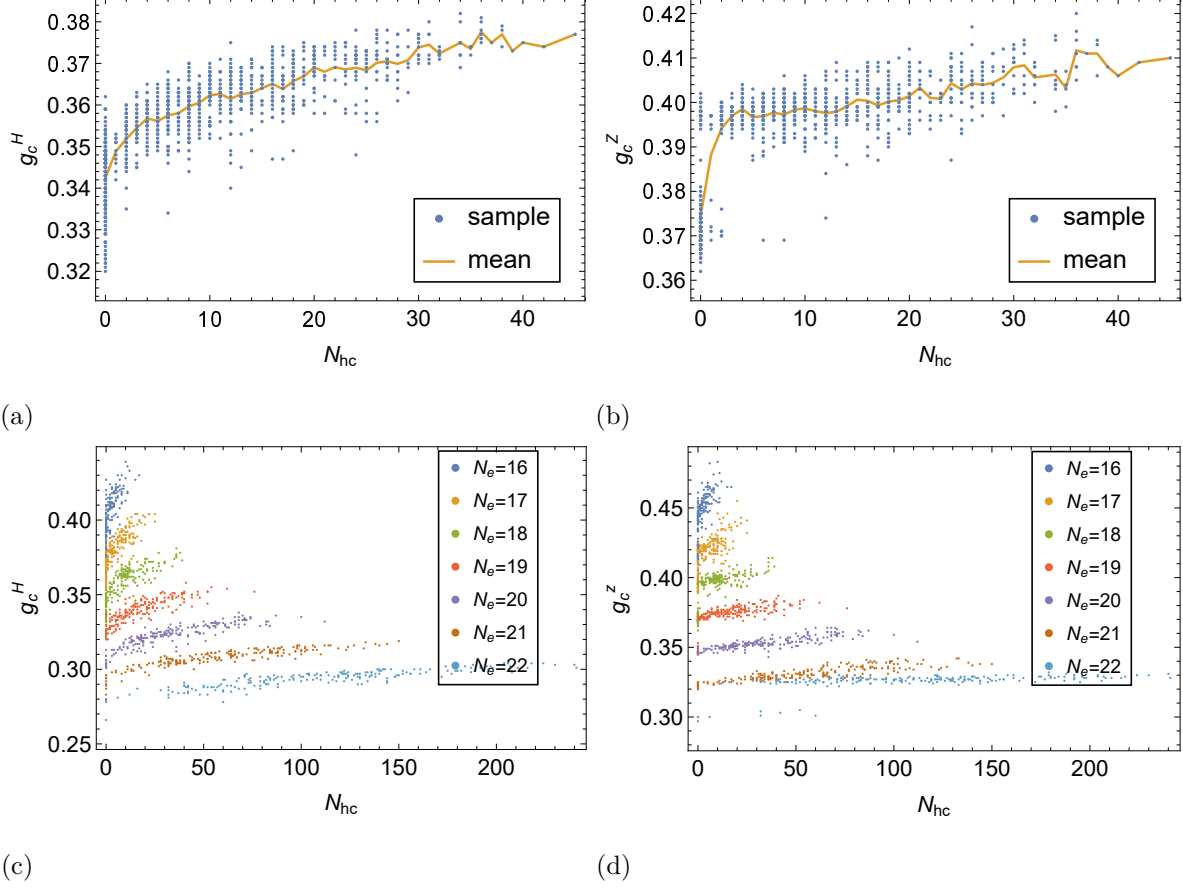


FIG. 6. Dependence of the critical parameters on N_{hc} . (a) Dependence of g_c^H on N_{hc} in graphs with $N_e = 18$. (b) Dependence of g_c^Z on N_{hc} in graphs with $N_e = 18$. (c) Dependence of g_c^H on N_{hc} in graphs with N_e varying from 16 to 22. (d) Dependence of g_c^Z on N_{hc} in graphs with N_e varying from 16 to 22.

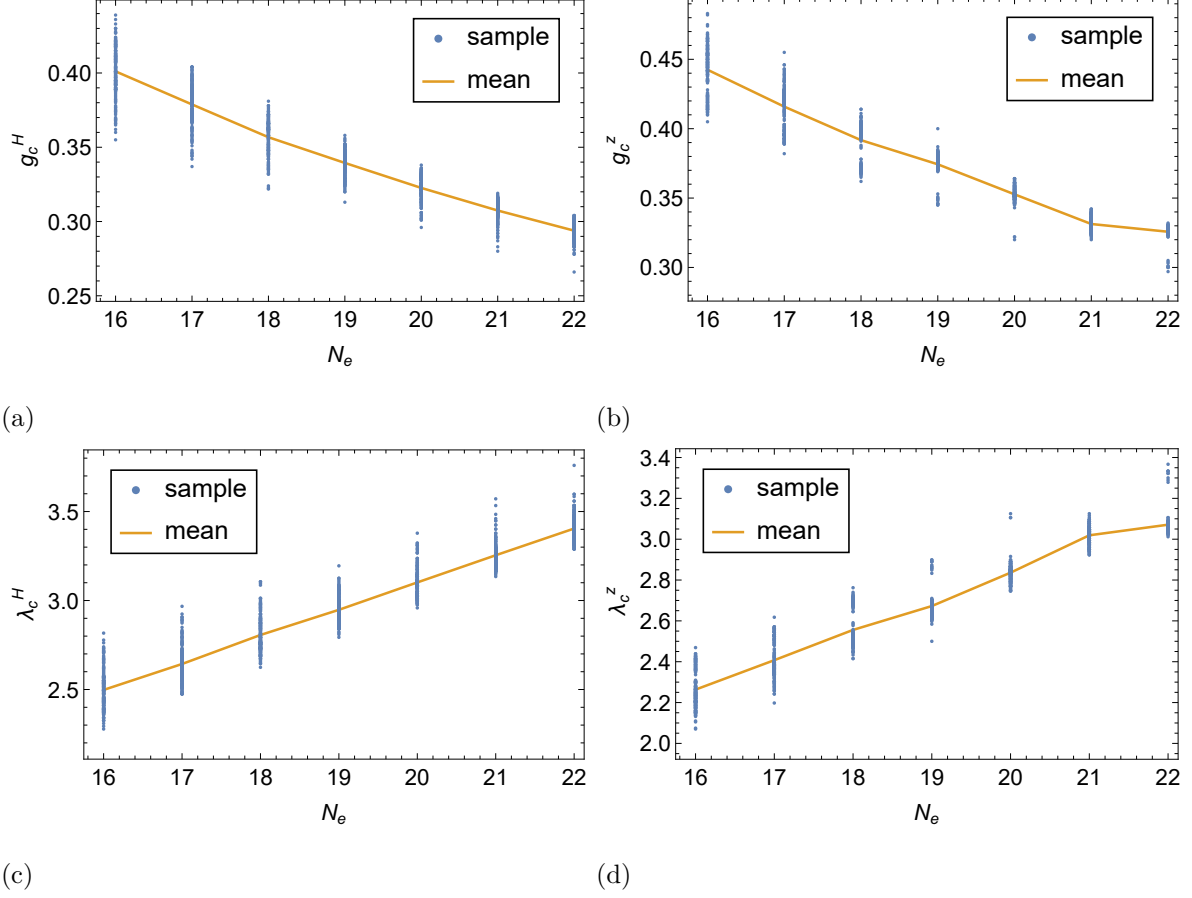


FIG. 7. The dependence of the critical parameters on N_e . (a) The dependence of g_c^H on N_e in the samples with N_e varying from 16 to 22. (b) The dependence of g_c^Z on N_e in the samples with N_e varying from 16 to 22. (c) The dependence of λ_c^H on N_e in the samples with N_e varying from 16 to 22. (d) The dependence of λ_c^Z on N_e in the samples with N_e varying from 16 to 22.

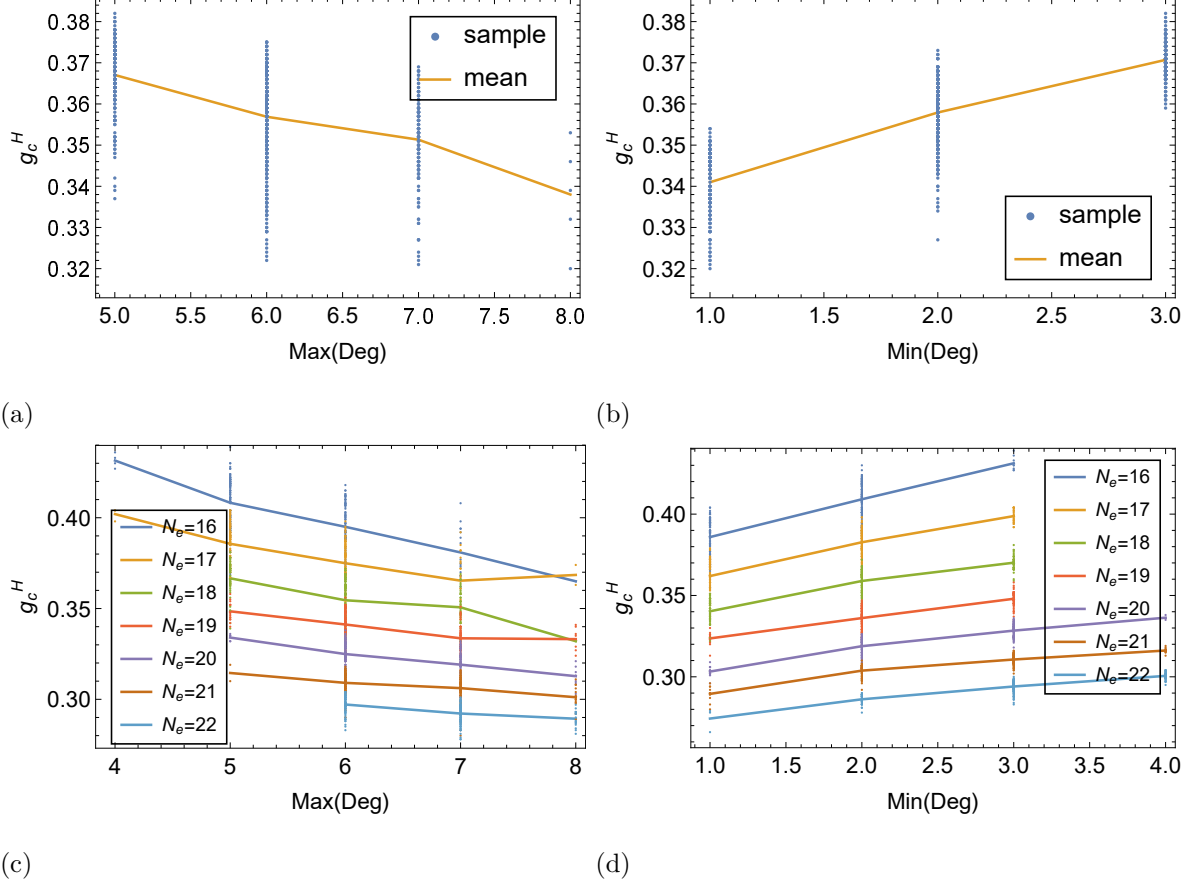


FIG. 8. The dependence of the critical parameters on the degree of vertices. (a) The dependence of g_c^H on $Max(Deg)$ in the samples with $N_e = 18$. (b) The dependence of g_c^H on $Min(Deg)$ in the samples with $N_e = 18$. (c) The dependence of g_c^H on $Max(Deg)$ in the samples with N_e varying from 16 to 22. (d) The dependence of g_c^Z on $Min(Deg)$ in the samples with N_e varying from 16 to 22.

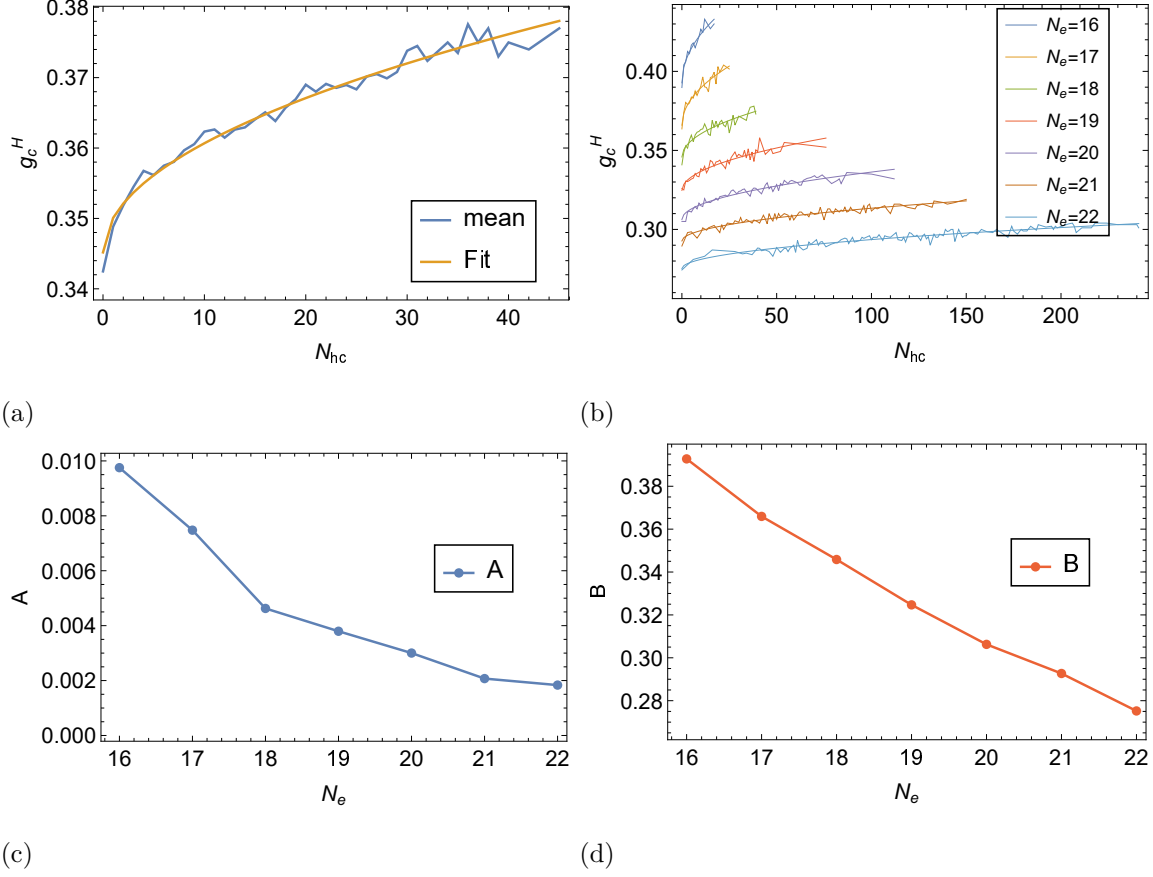


FIG. 9. The average value of g_c^H as a function of N_{hc} , fitted by $g_c^H = A\sqrt{N_{hc}} + B$. (a) The samples with $N_e = 18$. $A = 0.0049005$, $B = 0.345178$. (b) The sample with N_e varying from 16 to 22, with A and B depending on N_e . (c) Dependence of A in (b) on N_e . (d) Dependence of B in (b) on N_e .

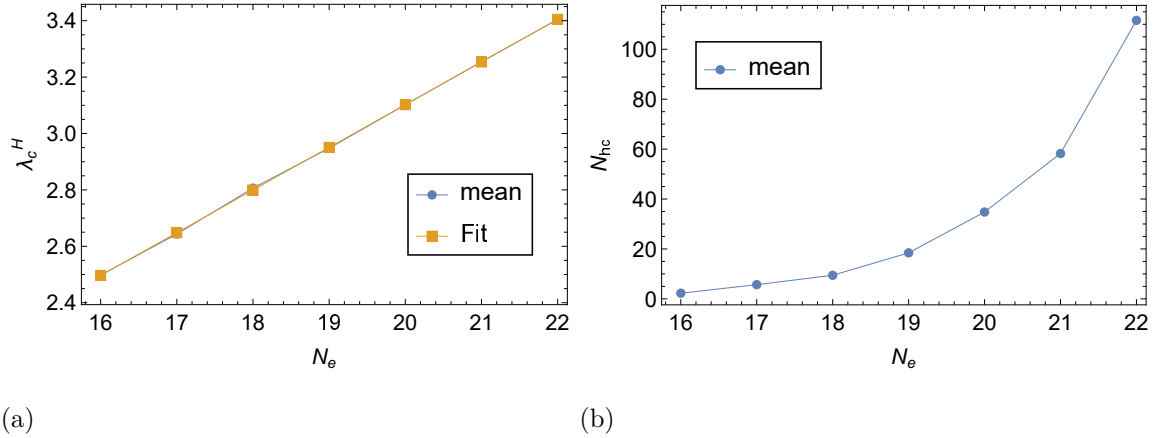


FIG. 10. (a) λ_c^H as a function of N_e , fitted by $\lambda_c^H = 0.1513 * N_e + 0.07536$. N_e varies from 16 to 22. (b) The dependence of the average value of N_{hc} on N_e , which varies from 16 to 22.